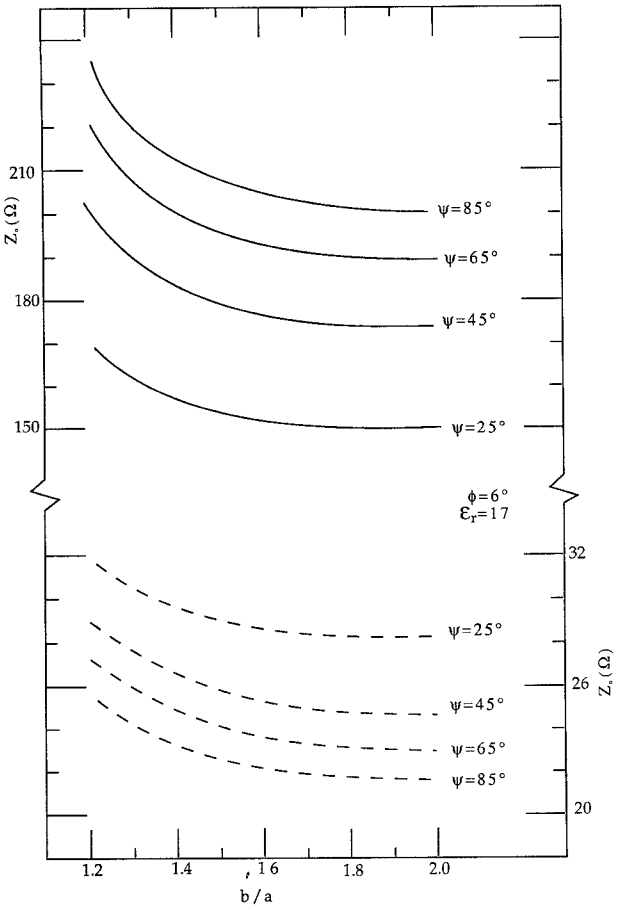

Fig. 3. Variation of the characteristic impedance with b/a and ψ.

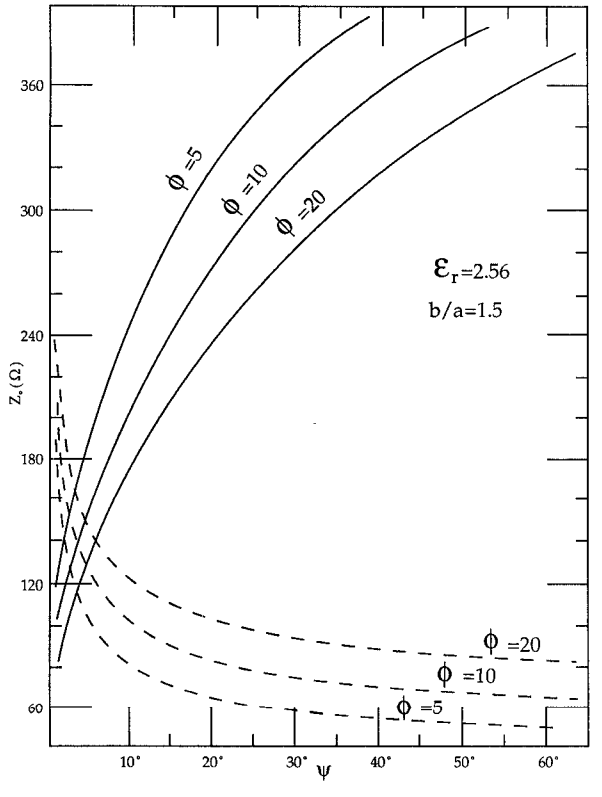

Fig. 4. Variation of the characteristic impedance with ψ and ϕ.

quasi-TEM analysis may be used for frequencies below X-band frequencies [7]. The solution is based on conformal transformation, and the validity of the method depends on the relative magnitudes of the ratio b/a and the arc strip width ϕ. These preliminary results suggest that the geometry shown in Fig. 1(b) is useful for low-impedance applications whereas the geometry of Fig. 1(a) provides a high-Z_0 transmission line. The feeding arrangement is very similar to that of a slotline, usually from a coaxial line.

References

[1] Y. C. Wang, "Cylindrical and cylindrically warped strip and microstrip lines," *IEEE Trans. Microwave Theory Tech.*, vol MTT-26, pp. 20–23, Jan 1978.

[2] K. K. Joshi and B. N. Das, "Analysis of elliptic and cylindrical striplines using Laplace's equation," *IEEE Trans. Microwave Theory Tech.*, vol. MTT-28, pp. 318–386, Apr. 1980.

[3] K. K. Joshi, J. S Rao, and B. N. Das, "Characteristic impedance of non-planar striplines," *Proc. Inst. Elec. Eng.*, pt. H, vol. 127, pp. 287–291, Aug. 1980.

[4] L. R. Zeng and Y V. Wang, "Accurate solution of elliptical and cylindrical strip and microstrip lines," *IEEE Trans. Microwave Theory Tech.*, vol. MTT-34, pp 259–265, Feb. 1986.

[5] C. J. Reddy and M. D. Deshpande, "Analysis of cylindrical stripline with multilayer dielectrics," *IEEE Trans. Microwave Theory Tech.*, vol. MTT-34, pp. 701–706, June 1986.

[6] C. P. Wen, "Coplanar waveguide: A surface strip transmission line suitable for non-reciprocal gyromagnetic device application," *IEEE Trans. Microwave Theory Tech.*, vol. MTT-17, pp. 1087–1090, Dec. 1969.

[7] K. C. Gupta, R. Garg, and I. J. Bahl, *Microstrip Lines and Slot Lines*. Dedham, MA: Artech House, 1980, pp. 262–275.

Spectral-Domain Immittance Approach for the Propagation Constants of Unilateral Finlines with Magnetized Ferrite Substrate

PEIJUE XUN

Abstract—**In this paper, the admittances of TM and TE modes in ferrite substrate are given, and the propagation constants for the forward and backward directions of the dominant mode in unilateral finlines with magnetized ferrite substrate are obtained. The solution is obtained by applying the transverse equivalent transmission line in the spectral domain and Galerkin's method. Numerical results are presented which can be used in designing a finline displacement isolator.**

I. Introduction

Recently, finlines have become attractive for millimeter-wave integrated circuit applications. Different types of finline configurations, such as unilateral, bilateral, and antipodal on isotropic substrates, have been extensively studied and employed in practice. Realization of nonreciprocal devices in finline techniques is also of interest in the millimeter-wave range because of the relative compactness and integrability of the devices compared to conventional ferrite-loaded waveguide. Beyer *et al.* have reported the experimental investigation of finline isolators and circulators [1], [2]. The theoretical treatment in [2] is also useful; however, it

Manuscript received December 19, 1988; revised April 10, 1989.

The author is with the High Energy Electronics Institute, University of Electronic Science and Technology of China, Chengdu, Sichuan, People's Republic of China.

IEEE Log Number 8929884

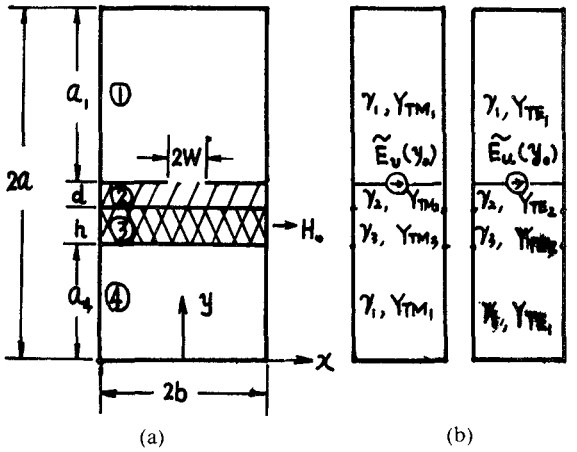

Fig. 1. (a) Cross-sectional view of a unilateral finline with a magnetized ferrite substrate (b) Equivalent transmission line for the TM-to-y and TE-to-y modes.

is based on the hybrid-mode field theory in the space domain and is complicated.

In the following, the spectral-domain immittance approach suggested by Itoh [3] is used to carry out an analysis of forward and backward wave propagation along unilateral finlines with magnetized ferrite substrates.

II. Admittances of TM and TE Modes in Ferrite Substrate

The unilateral finline to be analyzed here is shown in Fig. 1(a), where the z axis is chosen to be the direction of wave propagation. When a ferrite sample is magnetized to saturation along the x axis, the permeability tensor of the ferrite in region ③ is given by

$$\bar{\bar{\mu}} = \begin{bmatrix} \mu_0 & 0 & 0 \\ 0 & \mu & -jk \\ 0 & jk & \mu \end{bmatrix} \tag{1}$$

with

$$\mu = \mu_0\left[1 + \frac{\gamma^2 H_0 M_0}{(\gamma H_0)^2 - \omega^2}\right] \qquad k = \mu_0 \frac{\gamma M_0 \omega}{\omega^2 - (\gamma H_0)^2} \tag{2}$$

where μ_0 is the free-space permeability, ω is the operating frequency, H_0 is the applied dc magnetic field, M_0 is the saturation magnetization of the ferrite, and γ is the gyromagnetic ratio.

Through mathematical operations of Maxwell's equation in ferrite, we can get

$$\frac{\partial^2 E_x}{\partial x^2} + \frac{\partial^2 E_x}{\partial y^2} + \frac{\partial^2 E_x}{\partial z^2} + \omega^2 \epsilon_0 \epsilon_F \mu_\perp E_x = \frac{\omega k \mu_0}{\mu} \frac{\partial H_x}{\partial x} \tag{3}$$

$$\frac{\mu_0}{\mu}\frac{\partial^2 H_x}{\partial x^2} + \frac{\partial^2 H_x}{\partial y^2} + \frac{\partial^2 H_x}{\partial z^2} + \omega^2 \mu_0 \epsilon_0 \epsilon_F H_x = -\frac{\omega k \epsilon_0 \epsilon_F}{\mu} \frac{\partial E_x}{\partial x} \tag{4}$$

where ϵ_0 is free-space dielectric constant, ϵ_F is the relative dielectric constant of the ferrite, and $\mu_\perp = \mu - k^2/\mu$. Combining (3) and (4), we obtain

$$L(E_x) = 0 \tag{5}$$

and

$$L(H_x) = 0 \tag{6}$$

where

$$L = \nabla_{tr}^4 + \frac{\mu_0}{\mu}\frac{\partial^4}{\partial x^4} + \left(1 + \frac{\mu_0}{\mu}\right)\nabla_{tr}^2 \frac{\partial^2}{\partial x^2} + \omega^2 \epsilon_0 \epsilon_F (\mu_0 + \mu_\perp)\nabla_{tr}^2 + 2\omega^2 \mu_0 \epsilon_0 \epsilon_F \frac{\partial^2}{\partial x^2} + \omega^4 \mu_0 \epsilon_0^2 \epsilon_F^2 \mu_\perp \tag{7}$$

with

$$\nabla_{tr}^2 = \frac{\partial^2}{\partial y^2} + \frac{\partial^2}{\partial z^2} = \frac{\partial^2}{\partial y^2} - \beta^2. \tag{8}$$

Since the finline being considered supports a hybrid field, both the TM-to-y and the TE-to-y mode would be present. Let the Fourier transform of the x field components be defined as

$$\tilde{E}_x(\alpha, y) = \int_{-b}^{b} E_x(x, y) e^{j\alpha x}\, dx \tag{9}$$

$$\tilde{H}_x(\alpha, y) = \int_{-b}^{b} H_x(x, y) e^{j\alpha x}\, dx \tag{10}$$

where α takes discrete values given by $\alpha = n\pi/b$ for odd modes and by $\alpha = (n + \frac{1}{2})\pi/b$ for even modes. Introducing (9) and (10) into (5) and (6), we obtain the admittances of TM and TE modes:

$$Y_{\mathrm{TM}} = \frac{j\omega \epsilon_0 \epsilon_F}{\gamma_F} \tag{11}$$

$$Y_{\mathrm{TE}} = \frac{\alpha^2(\mu^2 - k^2) + \mu_0 \mu \beta^2}{j\omega \mu_0 (\mu^2 - k^2)(\alpha^2 + \beta^2)}\gamma_F + \frac{k\beta}{j\omega(\mu^2 - k^2)} \tag{12}$$

with

$$\gamma_F = \sqrt{\beta^2 - \tfrac{1}{2}\left[\omega^2 \epsilon_0 \epsilon_F (\mu_0 + \mu_\perp) - \left(1 + \frac{\mu_0}{\mu}\right)\alpha^2\right] \pm Q}$$

$$Q = \sqrt{\tfrac{1}{4}\left[\omega^2 \epsilon_0 \epsilon_F (\mu_\perp - \mu_0) - \left(1 - \frac{\mu_0}{\mu}\right)\alpha^2\right]^2 + \omega^2 \mu_0 \epsilon_0 \epsilon_F \alpha^2 \frac{k^2}{\mu^2}}. \tag{13}$$

We then use the spectral-domain immittance approach to calculate the propagation constants for the forward and backward directions of finlines with magnetized ferrite substrate.

III. Determinantal Equation

The current densities and electric fields of Fig. 1(b) are

$$\begin{bmatrix} Y_{11} & Y_{12} \\ Y_{21} & Y_{22} \end{bmatrix}\begin{bmatrix} \tilde{E}_x(\alpha, y_0) \\ \tilde{E}_z(\alpha, y_0) \end{bmatrix} = \begin{bmatrix} \tilde{J}_x(\alpha, y_0) \\ \tilde{J}_z(\alpha, y_0) \end{bmatrix} \tag{14a}$$

where

$$Y_{11} = Y^e N_x^2 + Y^h N_z^2 \tag{14b}$$

$$Y_{12} = Y_{21} = (Y^e - Y^h) N_x N_z \tag{14c}$$

$$Y_{22} = Y^e N_z^2 + Y^h N_x^2 \tag{14d}$$

$$y_0 = a_2 + h + d \tag{14e}$$

with

$$N_x = \alpha/\sqrt{\alpha^2 + \beta^2} \qquad N_z = \beta/\sqrt{\alpha^2 + \beta^2}. \tag{14f}$$

Here, Y^e and Y^h are the driving-point admittances at interface 1 (see Fig. 1(a)) for the TM and TE modes, respectively, and are

given by

$$Y^e = Y_{TM_1}\coth\gamma_1 a_1 + Y_{TM_2}\frac{A\coth\gamma_2 d + B}{A + B\coth\gamma_2 d} \tag{15a}$$

with

$$A = Y_{TM_3}^2 + Y_{TM_1}Y_{TM_3}\coth\gamma_1 a_2\cdot\coth\gamma_3 h \tag{15b}$$

$$B = Y_{TM_2}\left(Y_{TM_1}\coth\gamma_1 a_2 + Y_{TM_3}\coth\gamma_3 h\right) \tag{15c}$$

and

$$Y^h = Y_{TE_1}\coth\gamma_1 a_1 + Y_{TE_2}\frac{C\coth\gamma_2 d + D}{C + D\coth\gamma_2 d} \tag{16a}$$

with

$$C = Y_{TE_3}^2 + Y_{TE_1}Y_{TE_3}\coth\gamma_1 a_2\cdot\coth\gamma_3 h \tag{16b}$$

$$D = Y_{TE_2}\left(Y_{TE_1}\coth\gamma_1 a_2 + Y_{TE_3}\coth\gamma_3 h\right). \tag{16c}$$

Y_{TM_1} and Y_{TE_1} are, respectively, the TM and TE admittances in the y direction in regions ① and ④ (the air regions), and γ_1 is the propagation constant in the y direction in the same regions. These three quantities are given by

$$Y_{TM_1} = \frac{j\omega\epsilon_0}{\gamma_1} \tag{17}$$

$$Y_{TE_1} = \frac{\gamma_1}{j\omega\mu_0} \tag{18}$$

$$\gamma_1 = \sqrt{\alpha^2 + \beta^2 - \omega^2\mu_0\epsilon_0}\,. \tag{19}$$

Expressions for Y_{TM_2}, Y_{TE_2}, and γ_2 in region ② (the dielectric region) are as follows:

$$Y_{TM_2} = \frac{j\omega\epsilon_0\epsilon_r}{\gamma_2} \tag{20}$$

$$Y_{TE_2} = \frac{\gamma_2}{j\omega\mu_0} \tag{21}$$

$$\gamma_2 = \sqrt{\alpha^2 + \beta^2 - \omega^2\mu_0\epsilon_0\epsilon_r}\,. \tag{22}$$

Similarly, $Y_{TM_3}Y_{TE_3}$, and γ_3 in region ③ (the ferrite region) are given by (11), (12), and (13).

Returning to (14a), the unknown aperture fields $\tilde{E}_x$ and $\tilde{E}_z$ are expanded in terms of known basis functions followed by the application of Parseval's theorem. This results in a homogeneous eigenvalue matrix equation [3].

IV. Numerical Results

The series expansions of the slot fields in the spectral domain are given by

$$\tilde{E}_x(\alpha) = \sum_{i=1}^{M} c_i\tilde{f}_{xi}(\alpha) \tag{23}$$

$$\tilde{E}_z(\alpha) = \sum_{j=1}^{N} d_j\tilde{f}_{zj}(\alpha) \tag{24}$$

where $\tilde{f}_{xi}$ and $\tilde{f}_{zj}$ are Fourier transforms of the basis functions f_{xi} and f_{zj}, which are chosen to be zero except for $|x| < w$.

The choice of the basis functions is important in achieving a highly efficient numerical solution, with minimum computer time, and convergence. Therefore, sinusidal functions as modified by "edge condition" term that satisfy the boundary conditions and whose Fourier transforms are available in closed forms are used as the basis functions in this paper. They are [6]

$$f_{xi}(x) = \frac{\cos\{(i-1)\pi(x/w+1)\}}{\sqrt{1-(x/w)^2}} \tag{25}$$

$$f_{zj}(x) = \frac{\sin\{j\pi(x/w+1)\}}{\sqrt{1-(x/w)^2}}. \tag{26}$$

Because the "edge condition" of the aperture electric field has been incorporated in the choice of basis functions, it is possible, even with matrices of extremely small size, to obtain quite accurate solution results. Numerical computation has been carried out, when $M = N = 1$, for finline structures consisting of WR-28 waveguide (26.5–40.0 GHz band) and a dielectric substrate ($\epsilon_r = 2.22$) of thickness 0.125 mm with a magnetized ferrite substrate ($\epsilon_F = 13.5$) located in the E plane of the waveguide. The applied dc magnetic field H_0 and the saturation magnetization M_0 are, respectively, 7.96 kA/cm and 3.98 kA/cm.

All waveguiding structures were assumed to be totally lossless. The results of the numerical computation are presented in Figs. 2, 3, and 4. In order to achieve very accurate solutions, 250 spectral terms were used. From Figs. 2 and 3, it can be observed that when the thickness of the ferrite substrate decreases, the

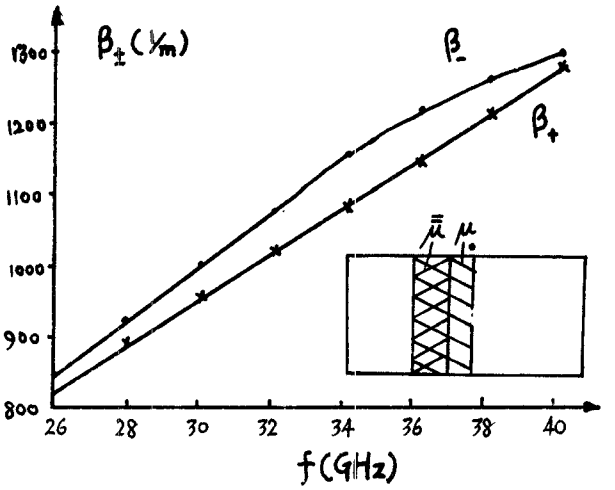

Fig. 2. Numerical results: $2a = 7.112$ mm, $2b = 3.556$ mm, $d = 0.125$ mm, $w/b = 0.1$, $h = 0.7$ mm

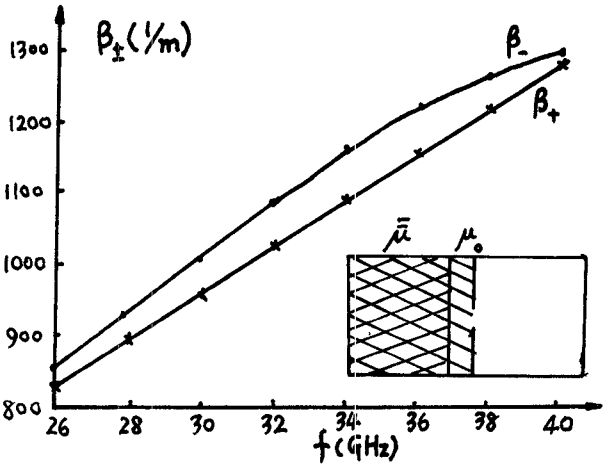

Fig. 3. Numerical results: $2a = 7.112$ mm, $2b = 3.556$ mm, $d = 0.125$ mm, $w/b = 0.1$, $h = 3.431$ mm.

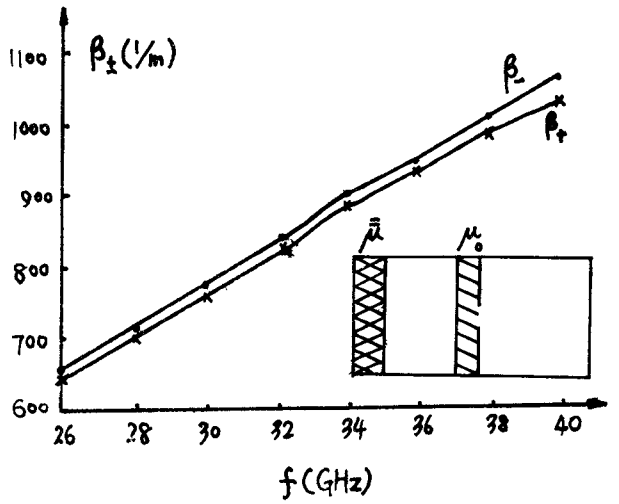

Fig 4 Numerical results: $2a = 7.112$ mm, $2b = 3.556$ mm, $d = 0.125$ mm, $w/b = 0.1$, $h = 1.0$ mm.

propagation constants and $(\beta_- - \beta_+)$ become smaller. Our computational results show that when the thickness of the ferrite substrate is larger than 1.0 mm β_+ and β_- increase very slowly. If the loss of ferrite materials is considered in designing isolators, the optimum thickness of the ferrite should be 1.0–1.2 mm.

From Fig. 4, we can see that when the ferrite substrate is located to the short side of the waveguide, the propagation constants and $(\beta_- - \beta_+)$ become smaller. This is because the propagating fields are concentrated in the neighborhood of the slot, and as the frequencies become larger the fields are more concentrated near the slot [8]. Other advantages of finline isolators are discussed in the literature [9].

Our computational results also show that as the thickness of dielectric substrates increases, the propagation constants and $(\beta_- - \beta_+)$ decrease.

V. Conclusions

The admittances of TM and TE modes in ferrite substrate are given by applying Maxwell's equations and Fourier transforms. The unilateral finline with magnetized ferrite substrate has been analyzed using the equivalent transmission line concept in the spectral domain in conjunction with Galerkin's method. Numerical results for propagation constants have been obtained and compared with the results available in the literature [2]. The results of forward and backward propagation constants are very useful in designing a displacement isolator with good quality. The field or power distributions are the most important information in designing a displacement type isolator. The author is currently investigating this, and the results will be reported in the near future.

Acknowledgment

The author wishes to thank Prof. K. J. Rao of the University of Electronic Science and Technology of China for his support and encouragement. The author dedicates this paper to his wife and daughter.

References

[1] A. Beyer and I Wolff, "A finline ferrite isolator and circulator for the *R*-band," presented at the 11th European Microwave Conf , Amsterdam, 1981

[2] A. Beyer and I Wolff, "Design of a millimeter-wave ferrite isolator at 28.5 GHz," *Proc. Inst. Elec Eng.*, pt. H, vol. 132, pp. 244–250, July 1985.

[3] T. Itoh, "Spectral domain immittance approach for dispersion characteristics of generalized printed transmission line," *IEEE Trans. Microwave Theory Tech.*, vol. MTT-28, pp. 733–736, July 1980.

[4] A. G. Gurevich, *Ferrites at Microwave Frequencies*. New York: Consultants Bureau, 1963.

[5] L. P. Schmidt, T. Itoh, and H. Hofmann, "Characteristics of unilateral finline structures with arbitrary located slots," *IEEE Trans. Microwave Theory Tech* , vol. MTT-29, pp. 352–355, Apr 1981

[6] L. P. Schmidt and T. Itoh, "Spectral domain analysis of dominant and higher order modes in fin-line," *IEEE Trans. Microwave Theory Tech.*, vol MTT-28, pp. 981–985, Sept. 1980.

[7] P. J. Xun, "The propagation constants of unilateral fin-line with magnetized ferrite substrate," presented at the Second Asia–Pacific Microwave Conf , Beijing, 1988.

[8] P. J. Xun, "Discrete Fourier transform for the field distributions of fin-line," *J. Univ. Electron. Sci. Technol. China*, to be published.

[9] A. Beyer and K. Solbach, "A new fin-line ferrite isolator for integrated millimeter-wave circuits," *IEEE Trans. Microwave Theory Tech.*, vol. MTT-29, pp. 1344–1348, Dec. 1981

Microstrip Ring Resonator Technique for Measuring Microwave Attenuation in High-T_c Superconducting Thin Films

JUNE H. TAKEMOTO, STUDENT MEMBER, IEEE, FLOYD K. OSHITA, STUDENT MEMBER, IEEE, HAROLD R. FETTERMAN, SENIOR MEMBER, IEEE, PAUL KOBRIN, AND EMILIO SOVERO, MEMBER, IEEE

***Abstract*—Microwave attenuation of high-T_c superconducting (HTS) films sputtered on MgO and ZrO_2 were measured using a microstrip ring resonator circuit. The results of Y–Ba–Cu–O and Bi–Sr–Ca–Cu–O resonators were compared to gold-plated resonators of identical design. The losses of superconducting and gold-plated films were determined from unloaded Q-factor measurements. The attenuation of Y–Ba–Cu–O film on a MgO substrate is approximately 31 percent lower than gold films at 6.6 GHz and 33 percent lower at 19.2 GHz for temperatures below 50 K. The approach of using microstrips to characterize microwave losses shows the usefulness of HTS films in integrated circuit technology.**

I. Introduction

The recent discovery of high-T_c superconductors (HTS's) has drawn considerable attention towards the possibility of using thin films in microwave integrated circuits. Zero dc resistivity and reduced microwave attenuation give HTS performance advantages over devices and circuits fabricated with conventional gold conductors. Numerous high-frequency measurements have been reported which characterize these new oxide superconductors at microwave and millimeter-wave frequencies using high-Q cavity resonators [1], [2] and stripline resonators [3]. In this paper we report results on microwave attenuation in Y–Ba–Cu–O (YBCO) and Bi–Sr–Ca–Cu–O (BSCCO) superconductors based on Q-factor measurements of microstrip ring resonators. To our knowledge this is the first reported implementation of superconducting microstrip, which demonstrates the applicability of fabricating

Manuscript received January 13, 1989; revised April 25, 1989

J. H. Takemoto was with the Electrical Engineering Department, University of California at Los Angeles, Los Angeles, CA 90024. She is now with TRW, MS R1/2170, One Space Park, Redondo Beach, CA 90278

F. K. Oshita and H. R. Fetterman are with the Electrical Engineering Department, University of California at Los Angeles, Los Angeles, CA 90024.

P. Kobrin and E. Sovero are with the Rockwell Science Center, Thousand Oaks, CA 91360

IEEE Log Number 8929928.